NUWC-NPT Technical Report 11,116
30 April 1999

Analysis of Velocity Measurements at NOTS Pier on San Clemente Island

Peter J. Hendricks
Torpedo Systems Technology Department

Naval Undersea Warfare Center Division
Newport, Rhode Island

PREFACE

This report was prepared under the Naval Undersea Warfare Center Research Assignment No. TD0976, principal investigator Paul R. Temple (Code 8213). The project was funded by the Office of Naval Research under Subsurface Nonacoustic Antisubmarine Warfare. The sponsoring activity is the Office of Naval Research, program manager, D. Johnson (ONR321SI).

The technical reviewer for this report was John R. Grant (Code 8233).

Reviewed and Approved: 30 April 1999

James C. S. Meng
Head, Torpedo Systems Technology Department

REPORT DOCUMENTATION PAGE

Form Approved
OMB No. 0704-0188

1. AGENCY USE ONLY *(Leave blank)*	2. REPORT DATE	3. REPORT TYPE AND DATES COVERED
	30 April 1999	

4. TITLE AND SUBTITLE

Analysis of Velocity Measurements at NOTS Pier on San Clemente Island

5. FUNDING NUMBERS

6. AUTHOR(S)

Peter J. Hendricks

7. PERFORMING ORGANIZATION NAME(S) AND ADDRESS(ES)

Naval Undersea Warfare Center Division
1176 Howell Street
Newport, RI 02841-1708

8. PERFORMING ORGANIZATION REPORT NUMBER

TR 11,116

9. SPONSORING/MONITORING AGENCY NAME(S) AND ADDRESS(ES)

Office of Naval Research
Ballston Centre Tower One
800 North Quincy Street
Arlington, VA 22217-5660

10. SPONSORING/MONITORING AGENCY REPORT NUMBER

11. SUPPLEMENTARY NOTES

12a. DISTRIBUTION/AVAILABILITY STATEMENT

Approved for public release; distribution is unlimited.

12b. DISTRIBUTION CODE

13. ABSTRACT (Maximum 200 words)

This report describes oceanographic observations at NOTS Pier on San Clemente Island, CA. Velocity measurements were made to assess the suitability of NOTS Pier for testing ocean turbulence sensors.

Measurements at NOTS Pier on San Clemente Island off the coast of Southern California show that the water velocities there consist of tidal currents and oscillations caused by surface waves. Tidal currents are parallel to the shoreline with frequencies that are mixed diurnal and semidiurnal with an rms amplitude of approximately 8 cm/s. Ocean swells (10- to 12-s period) and wind waves (3- to 5-s period) induce periodic horizontal and vertical velocities with rms amplitudes of 5 cm/s and 1 cm/s, respectively, under quiet conditions.

Direct measurement of small-scale velocities with high-frequency current meters indicates that the velocity field under the pier is consistent with anisotropic turbulence. Using a model of "frozen field" turbulence in an oscillating mean flow, estimates of the turbulent dissipation rate are $\varepsilon_u = 1.1 \times 10^{-5}$ m^2/s^3 based on the horizontal velocity spectrum and $\varepsilon_w = 1.1 \times 10^{-6}$ m^2/s^3 for the vertical.

14. SUBJECT TERMS			15. NUMBER OF PAGES
Acoustic Doppler Current Profiler	Acoustic Doppler Velocimeter	Modular Acoustic Velocity Sensor	37
Nonacoustic Antisubmarine Warfare	Ocean Turbulence Sensor	Sound Velocity Measurements	16. PRICE CODE

17. SECURITY CLASSIFICATION OF REPORT	18. SECURITY CLASSIFICATION OF THIS PAGE	19. SECURITY CLASSIFICATION OF ABSTRACT	20. LIMITATION OF ABSTRACT
Unclassified	Unclassified	Unclassified	SAR

TABLE OF CONTENTS

LIST OF ILLUSTRATIONS

LIST OF ILLUSTRATIONS (Cont'd)

LIST OF TABLES

ANALYSIS OF VELOCITY MEASUREMENTS AT NOTS PIER ON SAN CLEMENTE ISLAND

INTRODUCTION

This report summarizes the results from two oceanographic surveys at the Naval Ordnance Test Station (NOTS) on San Clemente Island, CA. The purpose of these surveys was to assess the suitability of NOTS Pier for testing ocean turbulence sensors.

San Clemente Island is located in the Southern California Bight approximately 50 miles west of San Diego, CA. San Clemente Island is owned and closely controlled by the U.S. Navy, which uses the island for a number of activities. This island provides a safe, secure environment for testing Navy equipment that may require shielding from public access. The measurements described in this report were conducted at or near a pier, known as NOTS Pier, on the east-facing shore on the northern part of the island.

A site visit was conducted on 25 January 1999 to assess the facilities at San Clemente Island and make some basic oceanographic measurements, particularly high-frequency velocity measurements in the water under the pier. The time available for measurements on the island was restricted to a short period because of the logistics of getting to and around on the island in a 1-day trip. Two commercially available instruments were used for the velocity measurements: a SonTek acoustic Doppler velocimeter (ADV) and a Nobska modular acoustic velocity sensor (MAVS). As the names imply, both instruments use acoustic techniques to measure velocity, but there are fundamental differences in the principles of operation. The ADV measures the Doppler shift from a high-frequency (10 MHz) acoustic beam backscattered from a single, small measurement volume with dimensions on the order of a centimeter. Signals from three receiving transducers are used to derive a single, three-component velocity vector within the volume. The measurements (pings) are repeated at high frequency (100 to 200 Hz) and averaged to form a single sample recorded every 40 ms (25 Hz). The averaging reduces the large statistical uncertainty inherent in each individual ping. The ADV is the primary candidate to be the reference sensor or standard of comparison for turbulence measurements with novel sensors, but there are no published data on its performance in very clear water with few scatterers such as is found near San Clemente Island. One of the principal goals of the site survey was to demonstrate the performance of the ADV in the clear water at this site.

The MAVS is based on the principle of acoustic travel time, whereby an acoustic pulse traveling between a stationary source and receiver arrives in a shorter time if there is a mean flow in the direction of propagation than if there is a mean flow in the opposite direction. This difference in travel time is proportional to the mean velocity averaged along the acoustic path. In the MAVS there are four 9.5-cm-long acoustic paths, each with counterpropagating acoustic pulses, arranged in an array to provide a redundant three-component velocity measurement. MAVS sends 1.75-MHz counterpropagating pulses every 20 ms, averaging and recording at an adjustable rate up to 6 samples per second. In normal operation, the principal noise source that

limits MAVS's high frequency performance is turbulence shed by the structural elements of the current meter and the supports for the acoustic transducers. If the mean currents are relatively weak, this noise is proportionally smaller. Because MAVS does not depend on acoustic scatterers in its operation, it should perform well in the clear waters near San Clemente Island.

There are actually two piers on the north end of San Clemente Islands that were considered as potential sites for testing, and measurements were made at both places. The other pier is located at Wilson Cove on the same coast as NOTS Pier about 2 miles to the northwest. Although the pier at Wilson Cove is newly refurbished and in much better condition than NOTS Pier, the water is not as deep under the Wilson Cove Pier (approximately 20 ft vs. 30 ft at NOTS). Also, the Wilson Cove site appears to be more open to incident waves, and the water is not as clear as the water under NOTS Pier. Measurements with ADV and MAVS made at Wilson Cove Pier confirmed that the waves there are more energetic than at NOTS Pier; the Wilson Cove data, however, are not discussed in this report.

Other Navy programs are using NOTS Pier for testing, and a data set containing acoustic Doppler current profiler (ADCP) and bottom-mounted pressure recorder data collected near NOTS Pier has been published (reference 1). These data will also be used to characterize the oceanographic environment at NOTS Pier.

VELOCITY MEASUREMENTS AT NOTS PIER

The current meters were suspended by cables or ropes from the walkway on the lower story of NOTS Pier about 100 ft from the end of the pier. The water depth at the site was estimated by sounding to be 20 ft, and the two meters were horizontally separated by about 8 ft. The measurements were made about 2 ½ hours after the low low tide. Three files were recorded with the ADV, and one high-rate file was recorded with MAVS. The parameters that describe these files are listed in table 1.

Table 1. NOTS Pier Velocity Measurements

Test/File	Sensor	Nominal Velocity Range (cm/s)	Sensor Depth (ft)	File Length (s)
NOTS1.ADV	ADV	±3	7	406
NOTS2.ADV	ADV	±3	14	731
NOTS3.ADV	ADV	±10	14	711
NP2.DAT	MAVS	±270	8	1100

ADV MEASUREMENTS

The nominal velocity range (see table 1) is an important parameter for the ADV in that it determines the maximum velocity that can be measured without an ambiguity in the velocity caused by overscaling; it also governs the sensitivity and intrinsic noise floor. Generally, the larger the velocity range, the higher the noise floor—though there are exceptions (reference 2). The term "nominal velocity range" is used because different velocity components have different ranges and noise floors. The velocity component parallel to the transmitted sound pulse, which was nominally vertical in the NOTS Pier deployment, has a velocity range and noise floor much lower than the two transverse components that were nominally horizontal at NOTS Pier. The relationship between the nominal range setting and the actual maximum velocities for individual components is shown in table 2, based on a table in a SonTek technical note.

Table 2. Velocity Ranges for SonTek ADV

ADV Velocity Range Setting (cm/s)	Maximum Horizontal Velocity (cm/s)	Maximum Vertical Velocity (cm/s)
± 3	± 30	± 8
± 10	± 60	± 15
± 30	± 120	± 30
± 100	± 300	± 75
± 250	± 360	± 90

Figure 1 shows the time series of the three velocity components from NOTS1.ADV. Every data point is plotted at the 25-Hz sample rate. The velocity components labeled "U" and "V" are nominally horizontal; the vertical velocity is labeled "W." The ADV does not have a compass, and it was suspended from a cable, free to rotate. Consequently, the absolute orientation of U and V with respect to the dock and whether the orientation changed with time is unknown.

The measured velocities, particularly the horizontal velocities, are periodic and have a mean near zero, as indicated by the labels on the graphs. Note that all velocities are in cm/s and the velocity scales for the horizontal components are larger than for the vertical velocity. The wild points that are evident in the plots are probably due to velocity ambiguities, although the maximum and minimum values listed on the right side of the plots indicate values in excess of the maximum values the manufacturer claims are possible for this range setting. Because of the apparent ambiguities, the data from file NOTS1.ADV will not be used in subsequent analyses.

The velocity time series from NOTS2.ADV are shown in figure 2, plotted using the same vertical scales as NOTS1.ADV, but with a longer time scale to accommodate the longer record. Even though the nominal velocity range is the same as NOTS1.ADV, no ambiguities are evident in the data from NOTS2.ADV. Most of the variance in these records is due to velocities induced by surface waves. The ADV was deeper for NOTS2.ADV (14 ft vs. 7 ft for NOTS1.ADV), and

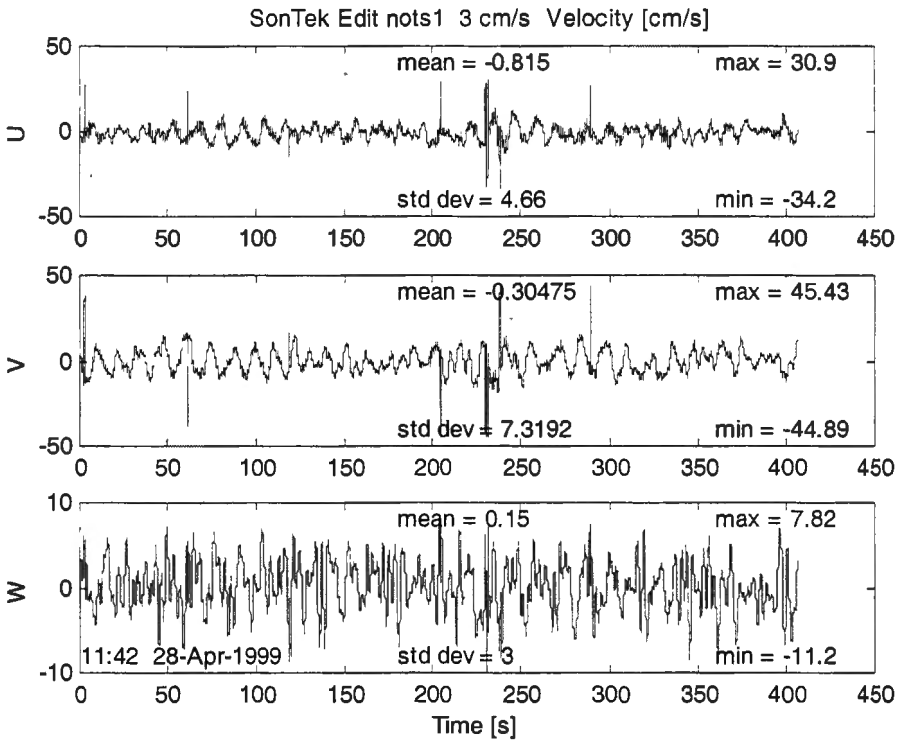

Figure 1. Velocity Time Series from NOTS1.ADV

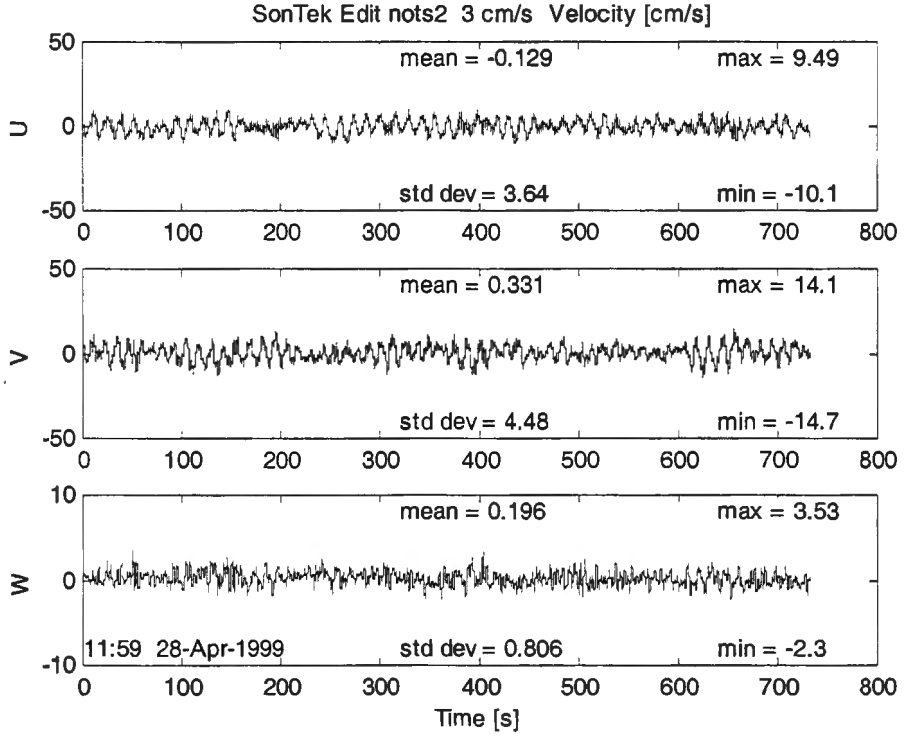

Figure 2. Velocity Time Series from NOTS2.ADV

the consequent greater attenuation of the surface wave-induced velocities may have eliminated the largest values that caused velocity ambiguities. The periodic nature of the velocity in NOTS2.ADV is very clear in figure 2 as is the difference in the amplitude and periodicity between the vertical and horizontal components. These characteristics can also be seen in the power spectra from NOTS2.ADV that are plotted in figure 3, where there are four curves that correspond to the two horizontal components (U and V), the vertical velocity (W), and the sum of the two horizontal components ($U + V$), where the power spectra of the two horizontal components have simply been added together. The $U + V$ spectrum is proportional to the horizontal kinetic energy and is used for comparison to MAVS velocity measurements, where the absolute geographic directions of U and V are similarly unknown. The legend in the upper right corner shows the rms, computed as the square root of the integrated power spectra (cm/s), and the peak value of the spectrum [(cm/s)^2/Hz]. Similarly, the rms for $U + V$ is effectively the amplitude (square root of the sum of the squares) of the two perpendicular vector components. The small differences between the rms velocities computed from the spectra and the standard deviations shown on the time series plots (figure 2) are due to the effects of finite data length and windowing in computing the spectra.

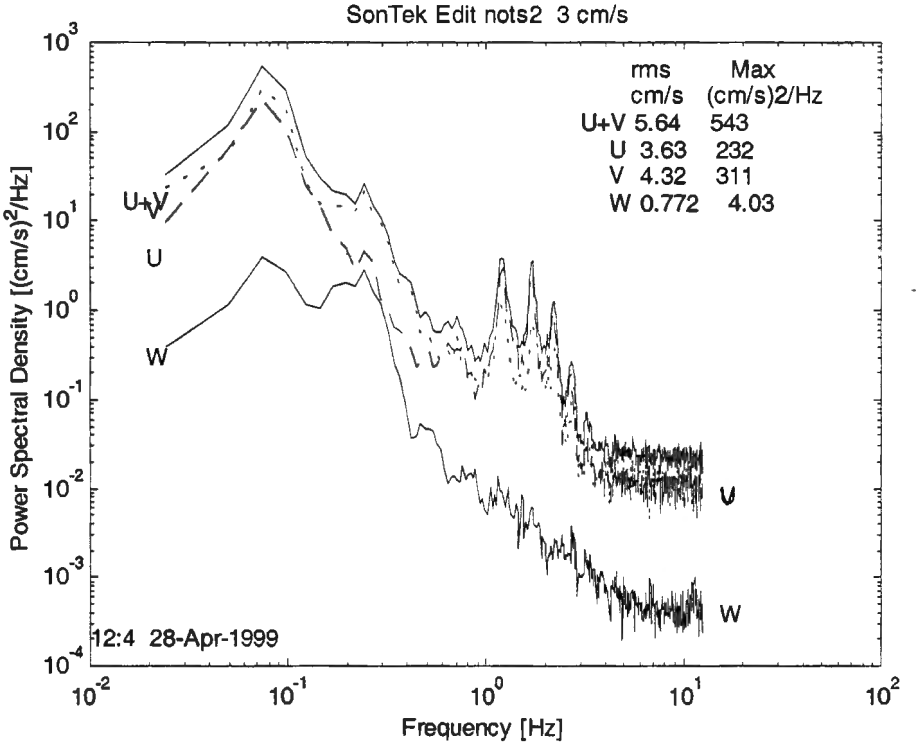

Figure 3. Velocity Spectra from NOTS2.ADV

The maxima in the spectra occur at a frequency of 0.1 Hz (10-s period)—corresponding to ocean wave swell. The maximum in the vertical velocity spectrum is almost two orders of magnitude lower than the horizontal, and the vertical velocity spectrum has a prominent secondary peak at about 0.3 Hz (3 s). These shorter period waves are probably wind waves,

which are generated by the action of local winds, as opposed to swell (swell ususally has a longer period and has been generated elsewhere). There are several additional peaks in the horizontal velocity spectra between 1 Hz and 4 Hz that are intermittent and tonal in nature. At times, these oscillations contribute as much as 1 to 2 cm/s to the rms velocity; they appear to be correlated with the periods of stronger swell activity and are tentatively attributed to strumming of the cable holding the current meter. If cable strumming is the cause of these oscillations, these oscillations will be eliminated when the meters are rigidly mounted in future tests.

To illustrate the effect of changing the velocity range, the time series and spectra from NOTS3.ADV are shown in figures 4 and 5, respectively. The NOTS3.ADV file began immediately after NOTS2.ADV ended, and the instrument was not moved; the only difference, then, between the two should have been the velocity range. Comparing the two data sets shows very little difference between them. Statistical properties such as mean and rms are very close, particularly for such short records. Although it is difficult to see from the spectra, flat parts of the spectra at high frequency are somewhat higher for NOTS3.ADV, where the nominal velocity range is 10 cm/s. The variances due to system noise have been computed from these spectra by taking the average between 5 Hz and 12.5 Hz and multipling the average value by the total bandwidth (12.5 Hz). The rms or square root of the variance has been compiled in table 3.

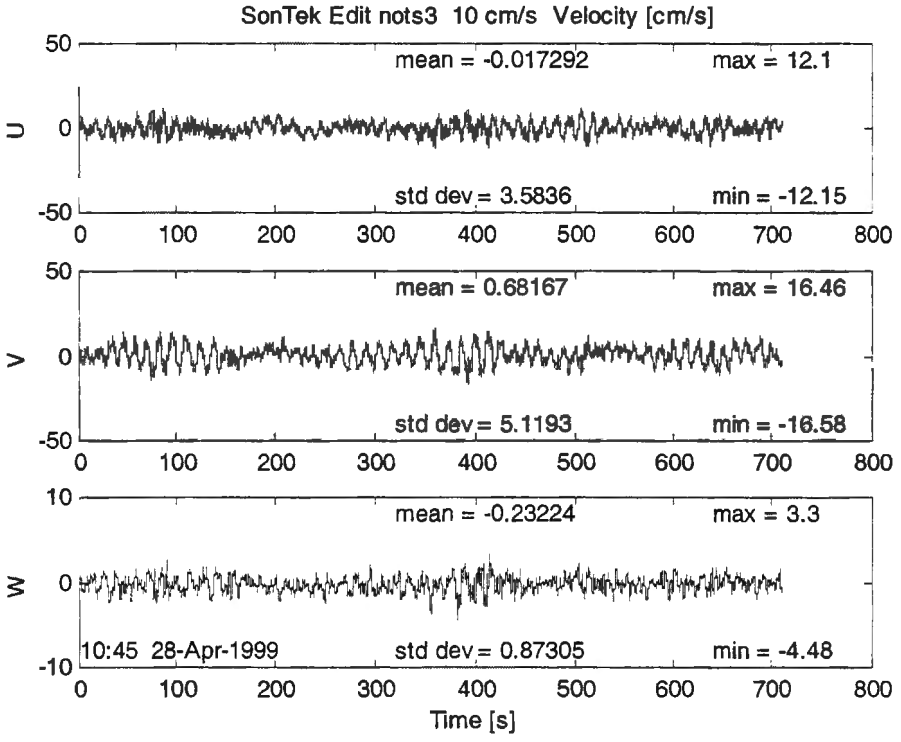

Figure 4. Velocity Time Series from NOTS3.ADV

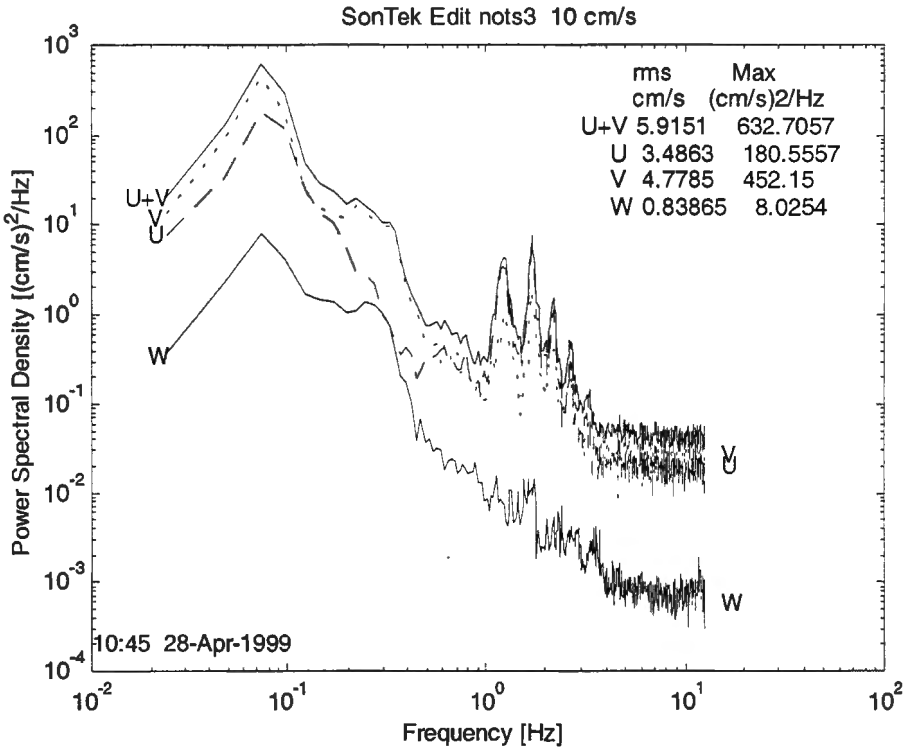

Figure 5. Velocity Spectra from NOTS3.ADV

Table 3. Noise Levels for SonTek ADV

Parameter	NOTS2.ADV	NOTS3.ADV
Nominal Velocity Range (cm/s)	± 3	± 10
Horizontal Velocity Noise Floor $(cm/s)^2/Hz$	0.030	0.042
Horizontal Velocity Noise Level (cm/s)	0.38	0.53
Vertical Velocity Noise Floor $(cm/s)^2/Hz$	.0064	.0088
Vertical Velocity Noise Level (cm/s)	0.08	0.11

When the measured noise levels in table 3 are compared with the actual maximum velocities in table 2 (not the nominal range), it appears that the rms noise increases by a factor of $\sqrt{2}$ when the actual range doubles from run NOTS2.ADV to NOTS3.ADV; that is, the noise variance doubles when the actual velocity range doubles. Reference 2 also found that the noise generally, but not always, increased with velocity range. Specifically in reference 2, the rms noise in still water for the nominal ranges ± 3 cm/s and ± 10 cm/s was essentially equal at 0.1 cm/s for the component corresponding to vertical (along the transmit beam), in reasonable agreement with the San Clemente Island measurements. Based on these observations, it is clear that the velocity range is an important parameter in the setup for the SonTek ADV.

MAVS MEASUREMENTS

The MAVS velocity measurements from NOTS Pier began near the end of NOTS3.ADV sampling interval. As indicated in table 1, the MAVS sensor was near the ADV, but probably at a shallower depth. Based on the MAVS pressure transducer, the average pressure was 2.4 decibar or the depth was 8 ft. Figures 6 and 7 show the time series and spectra from MAVS.

The MAVS velocity measurements are nearly identical to the ADV measurements with a few exceptions. The first difference is the mean velocity (U = -5.8 cm/s, V = -10.1 cm/s) in the MAVS measurements versus much smaller values for the ADV. This mean velocity is due to a zero offset in the MAVS. For a proper deployment, the MAVS should be set in still water to record zero-velocity values and the measured still water velocities should be used compensate for the offsets. For the San Clemente Island site visit, neither the time nor the facilities were available for zero-offset calibration. As a result, the means are unreliable, but the fluctuations should be properly represented. The second difference is that the rms vertical velocity measured by MAVS is somewhat greater than the ADV vertical velocity (1.2 cm/s vs. 0.8 cm/s). MAVS was shallower than the ADV, and there was less attenuation of vertical velocity, particularly for the higher frequency waves. This hypothesis is confirmed by comparing the vertical velocity spectrum from MAVS to the ADV spectrum and noting the peak at 0.3 Hz is much higher in the MAVS, where it is, in fact, slightly higher that the 0.1-Hz peak, which dominates the ADV vertical velocity spectrum. Lower frequency horizontal velocities are not attenuated with depth as rapidly as higher frequency vertical velocities. A more detailed discussion of surface waves and the velocities associated with them can be found in the appendix. The last major difference between the MAVS and ADV spectra is that there is no evidence in MAVS of the 1- to 4-Hz oscillations that were found in the ADV spectra, where it was attributed to cable strumming. MAVS was mounted in a stainless steel cage and supported by a rope, making it less susceptible to these tonal vibrations.

Otherwise the ADV and MAVS velocity measurements give nearly identical results. The rms horizontal velocity is within 5 percent, and the spectra are statistically indistinguishable, except for the three noted differences. Figure 8 compares the horizontal and vertical velocity spectra for the MAVS (solid line) and the ADV (dotted line).

The MAVS pressure sensor also recorded periodic oscillations attributed to the surface waves as shown in figures 6 and 7. The appendix shows that the pressure, horizontal velocity, and vertical velocity measurements from MAVS are consistent with surface waves with a 10-s period and an amplitude of 5 cm to 6 cm (height of 10 cm to 12 cm).

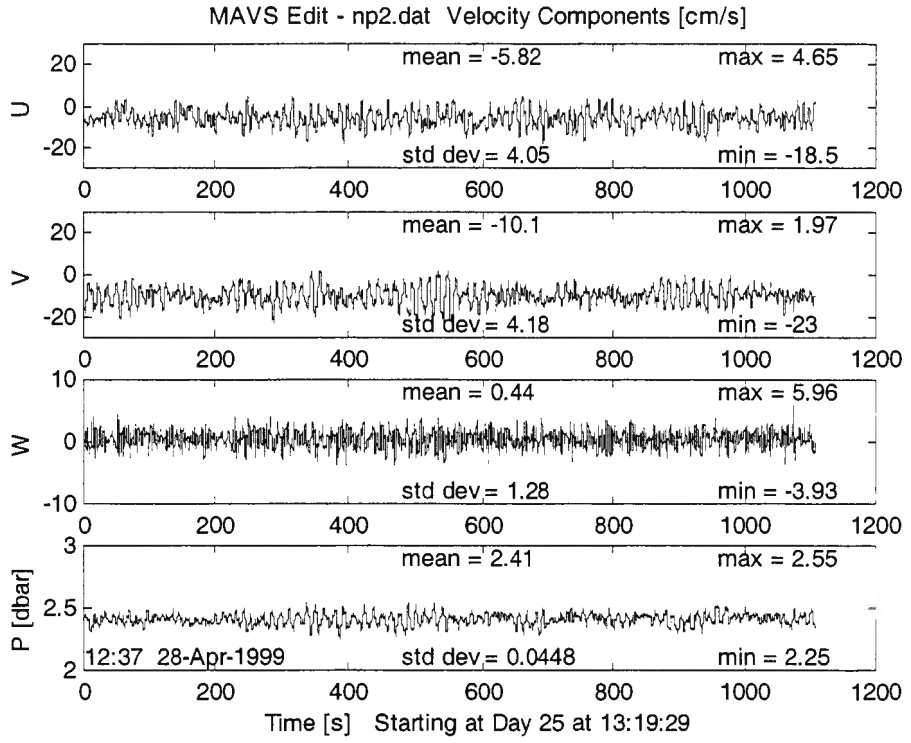

Figure 6. Velocity and Pressure Time Series from MAVS at NOTS Pier

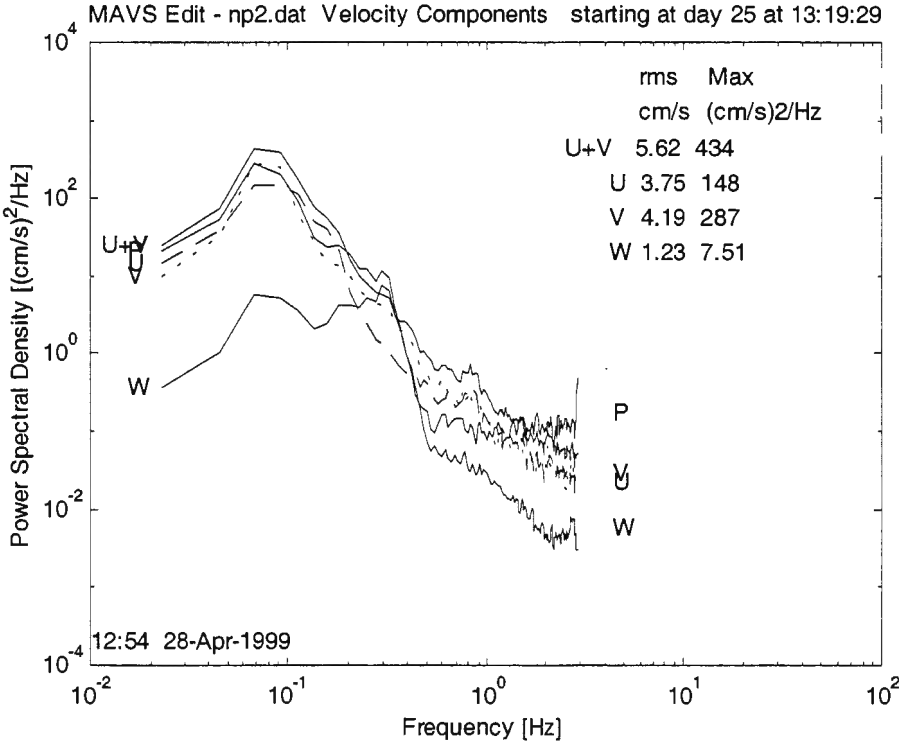

Figure 7. Velocity and Pressure Spectra from MAVS at NOTS Pier (the pressure scale is arbitrary)

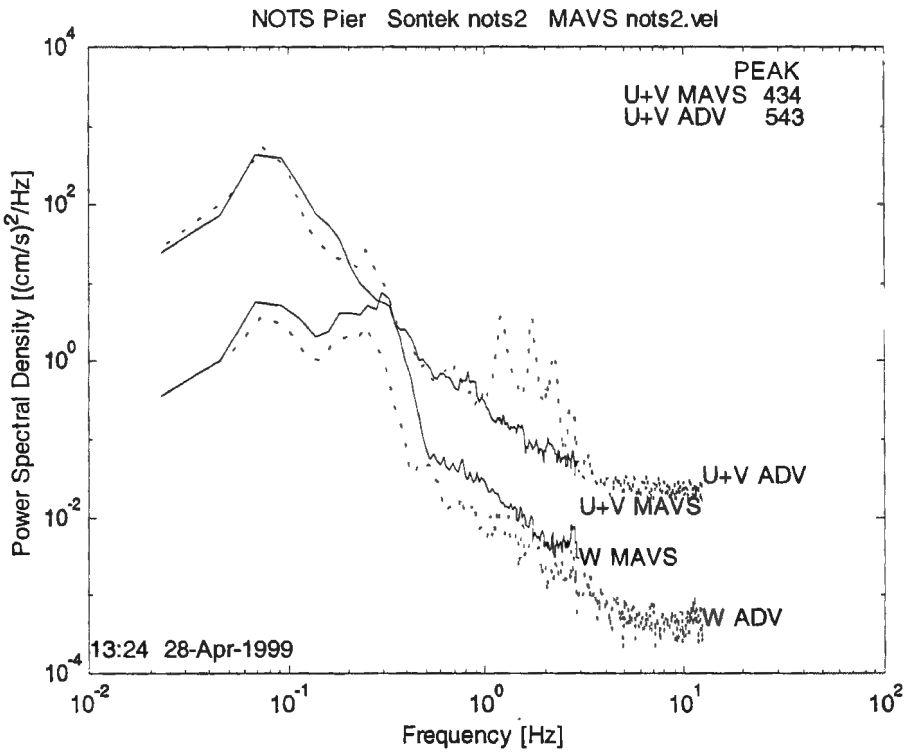

Figure 8. Comparison of Velocity Spectra for MAVS and ADV

TURBULENT VELOCITIES

The energy dissipation rate in a turbulent flow is the rate at which the flow loses turbulent kinetic energy by the action of viscosity. If the turbulent flow can be represented by a continuous spectrum where turbulent kinetic energy cascades from larger scales to smaller scales until the energy is ultimately dissipated by viscosity, then the dissipation rate ε is of order

$$\varepsilon \approx \frac{u^3}{l},$$

where u is the characteristic velocity of the energy containing turbulent eddies, and l is their length scale. While it is tempting to use the measured rms velocity for the velocity scale in estimating the dissipation rate, the major component of the rms at NOTS Pier is due to wave motion, which is irrotational and inherently nonturbulent and not dissipative. When the Reynolds number is high enough and the effects of stratification are taken into account, turbulent velocity spectra have a characteristic –5/3 power-law dependence on wave number, although such a spectrum is not a sufficient condition for turbulent flow. In the MAVS data, both horizontal and vertical velocity spectra have slopes that are indistinguishable from –5/3 in the range $0.5 < f < 2$ Hz, though these are frequency spectra rather than wave number spectra. In addition, the ADV vertical velocity spectrum has a similar slope at the same frequencies, but the horizontal velocities are contaminated by cable strumming in this frequency range. (There is

some indication from the ADV that the –5/3 range may extend to frequencies higher than 2 Hz before the spectrum is obscured by white noise. See figure 4.) Fitting a straight line with slope -5/3 to the MAVS velocity spectra in figure 7 gives the following equations for the spectra for the frequency $0.5 < f < 2$ Hz:

$$\textit{horizontal velocity} = S_u(f) = S_v(f) = 0.15 f^{-\frac{5}{3}} \quad (cm/s)^2/Hz,$$

$$\textit{vertical velocity} = S_w(f) = 0.03 f^{-\frac{5}{3}} \quad (cm/s)^2/Hz.$$

In many cases, it is possible to convert a measured frequency spectrum to a wave number, assuming that the sensor is moving through the fluid so rapidly that the turbulent velocity field does not change appreciably during the time of measurement. In that case, $u(t)$ is equivalent to $u(x/U)$, where U is the velocity of the sensor. This approximation is known as Taylor's hypothesis or the frozen-field approximation. These assumptions also imply $U >> u$. In the NOTS Pier case, the turbulent flow is advected back and forth past the sensors by the nearly horizontal velocity induced by the low-frequency wave motion. While it may be tenuous to apply Taylor's hypothesis to an oscillating flow, it does appear that U_{rms} associated with the wave motion is much greater than the turbulent velocities. With these caveats, an effective wave number $k^* = f/U_{rms}$ can be defined, and the spectra in terms of the effective wave number can be rewritten; i.e.,

$$S_u^*(k^*) = U_{rms} S_u(f/U_{rms}) \quad (cm/s)^2/(cycle/m),$$
$$S_w^*(k^*) = U_{rms} S_w(f/U_{rms}) \quad (cm/s)^2/(cycle/m)$$

in the wave number band ($0.5/U_{rms} < k^* < 2/U_{rms}$ cycles/m) when U_{rms} is expressed as m/s. From the MAVS and ADV measurements at NOTS Pier, $U_{rms} \sim 0.056$ m/s, and

$$S_u^*(k^*) = 8.4x10^{-3} k^{*-\frac{5}{3}} \quad (cm/s)^2/(cycle/m)$$
$$S_w^*(k^*) = 1.7x10^{-3} k^{*-\frac{5}{3}} \quad (cm/s)^2/(cycle/m)$$

for $9 < k^* < 36$ cycles/m.

The turbulent spectrum may extend to wave numbers lower than 9 cycles/meter, but the -5/3 power-law dependence is masked by the more energetic, irrotational wave velocities. The most likely source of the turbulence near NOTS Pier, particularly away from the surface and the bottom, is the interaction of the wave motions with the pilings and other pier structures, suggesting a minimum wave number of order $k^*_{min} \sim f_{10} / U_{rms} = 2$ cycles/m, where $\mathbf{f}_{10} = 1/10$ Hz is the frequency of the dominant wave velocities. By using this value of the minimum wave

number, the rms turbulent velocity can be estimated by integrating the spectrum, using the -5/3 power straight-line fit, to calculate the variance; i.e.,

$$\sigma^2_{u,t} = \int_{k^*_{min}}^{k^*_{max}} S^*_u(k^*)dk^* = 0.94\ (cm/s)^2$$

$$\sigma^2_{w,t} = \int_{k^*_{min}}^{k^*_{max}} S^*_w(k^*)dk^* = 0.19\ (cm/s)^2,$$

and the corresponding turbulent rms velocities are $u_{rms,t} = 0.97$ cm/s, and $w_{rms,t} = 0.43$ cm/s. The characteristic length scale of the wave-induced velocity is $l = U_{rms}/2\pi f_{10} = 0.08$ m. By using these values, the estimated dissipation rates are $\varepsilon_u = 1.1 \times 10^{-5}$ m^2/s^3 based on the horizontal velocity spectrum, and $\varepsilon_w = 1.0 \times 10^{-6}$ m^2/s^3 based on the vertical. If the turbulence is generated by interaction with the pilings, then the length scale associated with these structures may be the appropriate scale for estimating the dissipation rates. Assuming the pier dimensions are of order $l_p \sim 0.3$ m, then estimated dissipation rates are somewhat smaller; i.e., $\varepsilon_u = 3.0 \times 10^{-6}$ m^2/s^3, and $\varepsilon_w = 2.7 \times 10^{-7}$ m^2/s^3.

High Reynolds number turbulence has a universal wave number spectrum in the inertial subrange and at higher wave numbers; it depends only on the turbulent dissipation rate and the viscosity. While there is no generally accepted analytic form for this spectrum, it has been measured in the ocean and reported in reference 3. Reference 4 has tabulated the universal spectra in dimensionless form. This universal spectrum can provide a basis for comparison to the velocity measurements at NOTS Pier. There are two separate, but related, forms of the universal spectrum depending on the relationship between the direction of the sensor motion and the direction of the velocity component. If the direction of the sensor is parallel to the velocity component, then the longitudinal spectrum is the appropriate spectrum; if the sensor motion is perpendicular to the velocity component, the transverse spectrum applies. For the NOTS measurements, if the oscillating "mean velocity" attributed to the swell is horizontal, then the two horizontal velocity spectra will be one longitudinal spectrum parallel to the direction of the swell-induced velocity and one transverse spectrum perpendicular to the direction of the swell velocity. The vertical velocity should be represented by the transverse spectrum. Unfortunately, the sensor alignment for the NOTS Pier measurement was not recorded or controlled because the instruments were hung from cables free to rotate. As a result, the relative direction of the swell velocities to the horizontal components is unknown. In any event, the numerical difference between the two longitudinal and transverse spectra is not great and the basic conclusions from this scaling analysis are not critically dependent on which is applicable. Figure 9 compares the average horizontal velocity spectrum from MAVS ($(U+V)/2$) to the universal longitudinal spectrum for several values of dissipation rate. The universal wave number spectra were converted to frequency spectra using $U_{rms} = 5.6$ cm/s. From this plot, it appears that the dissipation rate based on the length scale associated with the swell, $l = U_{rms}/2\pi f_{10} = 0.08$ m, is close to the value $\varepsilon_u = 1.1 \times 10^{-5}$ m^2/s^3 estimated earlier for the frequency band $0.5 < f < 2$ Hz, while the estimate based on the pier dimensions is low.

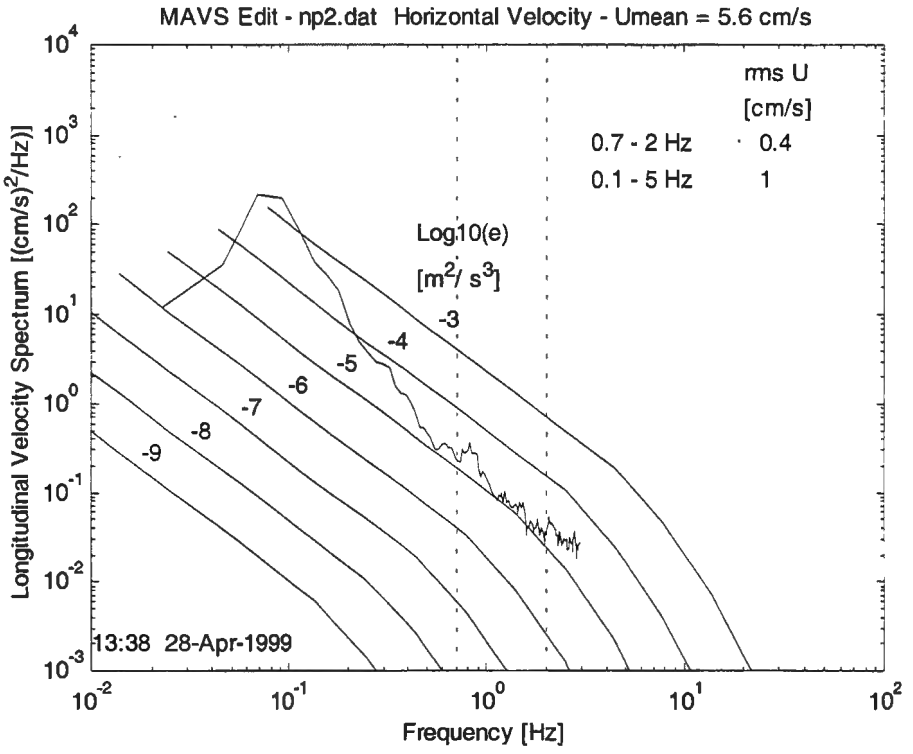

Figure 9. Comparison of MAVS Horizontal Velocity to Universal Longitudinal Velocity Spectrum

Similarly, figure 10 compares the MAVS vertical velocity spectrum to a series of universal transverse velocity spectra. Again, the earlier estimate of $\varepsilon_w = 1.0 \times 10^{-6}$ m^2/s^3 (based on the swell-length scale) is a close approximation to the spectrum over the range of applicability, and the estimate based on the pier dimensions is low. The measured spectrum, however, does diverge from the universal spectrum at the higher end for the frequency range—probably because of noise in the vertical velocity measurements. Also note that the universal spectra begin to drop off from the -5/3 slope because of the effects of viscosity for these frequencies and dissipation rates. This result also indicates that earlier estimates of rms turbulent velocities based on a -5/3 spectrum extrapolated to 0.1 Hz are reasonably accurate. Because the universal turbulent spectra are based on measurements of turbulence in the open ocean (reference 3), the agreement suggests the turbulence found under NOTS Pier will be representative of such ocean turbulence (at least up to its second moment) and a good test environment for the turbulence sensor testing. Figures 9 and 10 also show the rms velocity calculated directly by integrating the spectrum over the frequency range indicated by the dotted lines. These rms velocities are then extrapolated to the frequency range $0.1 < f < 10$ Hz using a -5/3 power law. The results are comparable to the earlier estimates based on a straight-line fit to the spectra. Comparable plots for the ADV are shown in figures 11 and 12, where noise limits the interval for direct calculation to $0.5 < f < 1$ Hz. The estimated broadband rms horizontal velocity for the ADV, however, is very close to MAVS, while the ADV rms vertical velocity is somewhat lower.

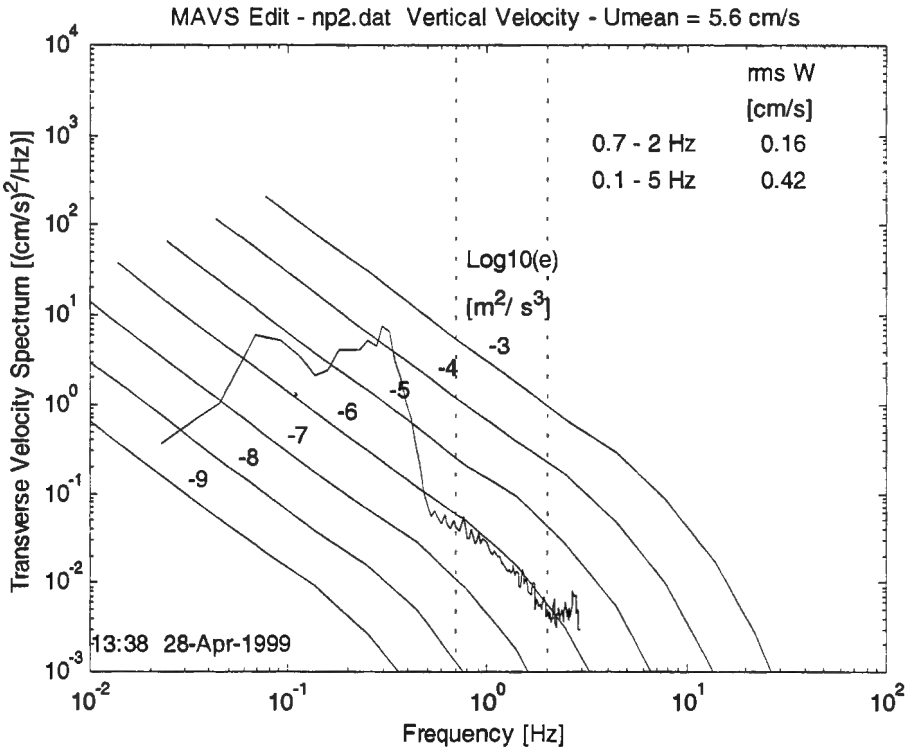

Figure 10. Comparison of MAVS Vertical Velocity to Universal Transverse Velocity Spectrum

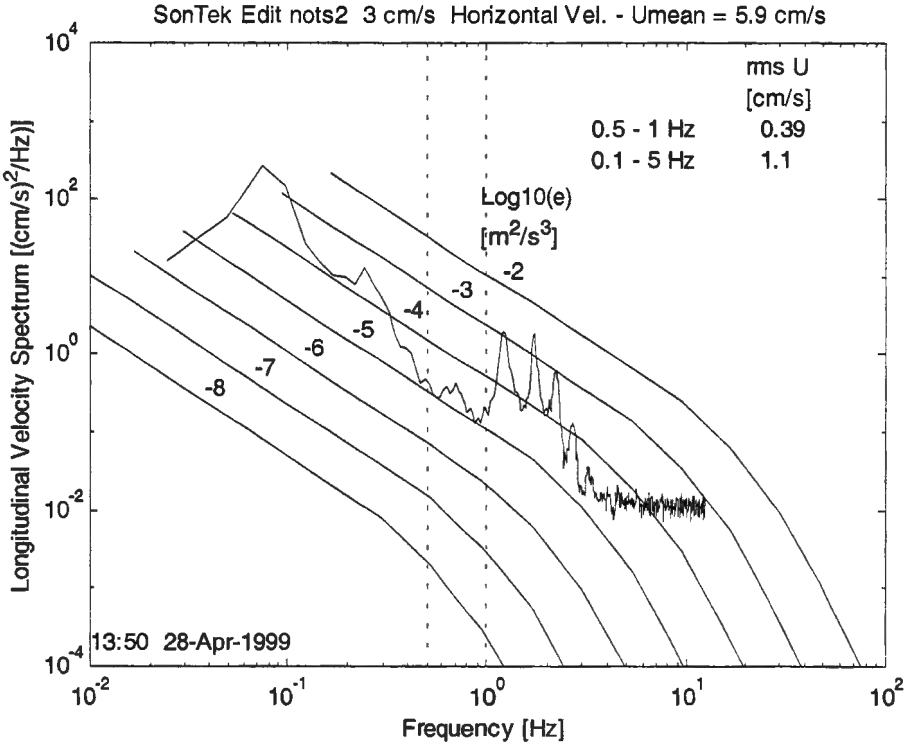

Figure 11. Comparison of ADV Horizontal Velocity to Universal Longitudinal Velocity Spectrum

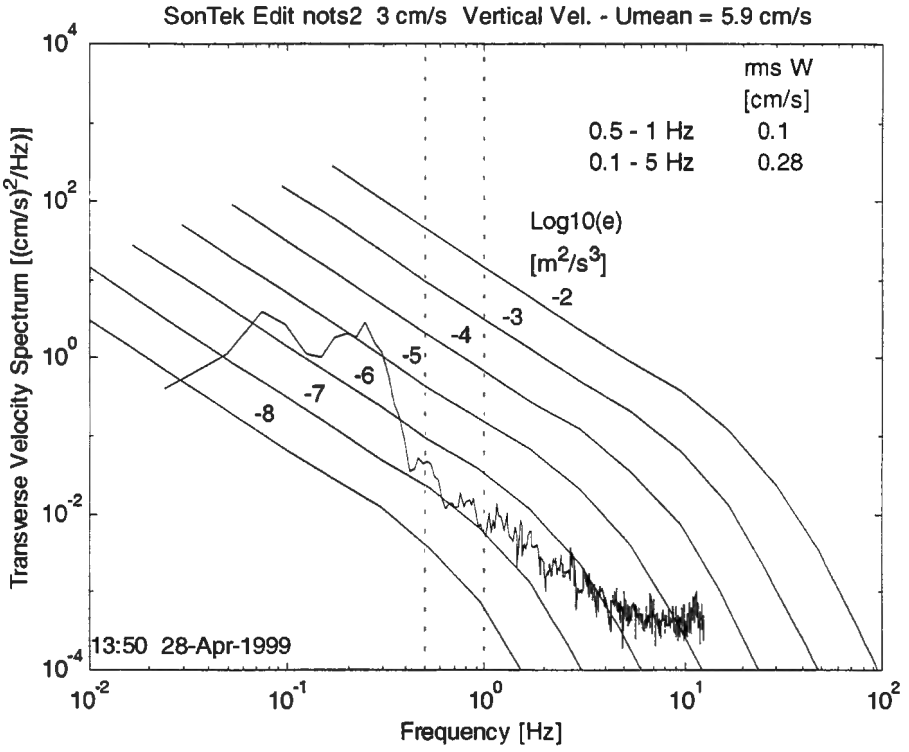

Figure 12. Comparison of ADV Vertical Velocity to Universal Transverse Velocity Spectrum

ACOUSTIC DOPPLER CURRENT PROFILER MEASUREMENTS

Extensive oceanographic and meteorological measurements—including data for several deployments of ADCPs, moored on the bottom, projecting upward, and attached to a boat looking down—were taken November through December 1998 near NOTS Pier (reference 1). This analysis focuses on the data from an ADCP (see table 4 for characteristics) on the bottom about 30 m off the end of NOTS Pier near the 15-m isobath.

Table 4. Specifications for ADCP Moored off NOTS Pier

Model	RDI Broadband Workhorse
Acoustic Frequency	600 kHz
Number of Beams	4
Beam Angle	20 °
Number of Bins	35
Bin Length	0.5 m
Blank after Transmit	0.3 m
Distance to First Bin	0.9 m
Transmit Length	0.5 m
Pings per Ensemble	30
Time per Ping	1.98 s
Record Length	30 days

ADCP measurements, like the ADV, have an inherent, large statistical uncertainty associated with the return from each ping. This error is random and can be reduced by averaging, whereby the variance from such averages is inversely proportional to the number of samples in the average. In processing the ADCP, samples are averaged in time and bins are averaged in the vertical to compute the velocity at a few layer depths. For this analysis, there are three average-layer depths, each 3.5 m thick (7 bins, each 0.5 m thick), located approximately 3 m, 6.5 m, and 10 m above the bottom. The hourly averaged velocities are plotted for the 1-month time period in figure 13. Each averaged velocity uses 12,600 pings, which reduces the random variations by about a factor of 100 in the rms velocity. Three traces are plotted in each panel for the three different depths, though it is often difficult to see three separate traces because the velocities are so nearly equal.

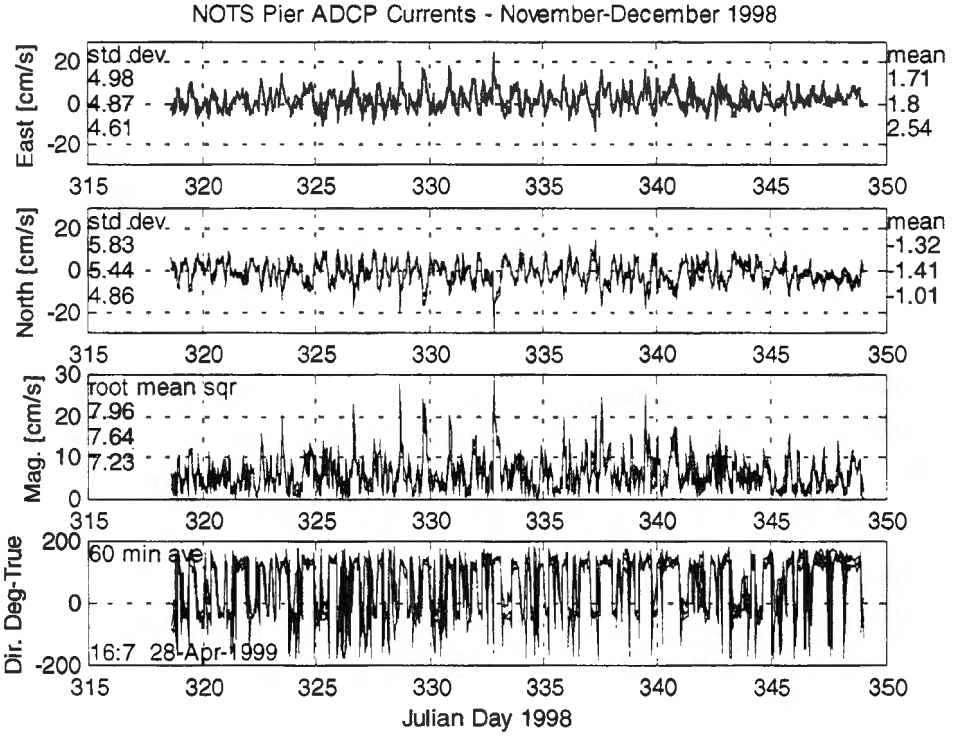

Figure 13. Hourly Average Currents off NOTS Pier (East component, north component, magnitude, and direction are plotted at 3, 6.5, and 10 m above the bottom.)

The currents in figure 13 are dominated by tidal components, which in the Southern California bight are characteristically a mixed tide that is mainly diurnal. The notations on the graphs show the means, standard deviations, and rms for the three depth levels in order of height above the bottom. It is clear that the long-term mean currents are weak, 1 to 2 cm/s, and the rms is 7 to 8 cm/s with peak values of 20 to 30 cm/s. The current direction plot in the bottom panel shows that the current direction is bimodal, indicating rectilinear back-and-forth motion. This motion is seen more clearly in figure 14 where the histogram of average direction is plotted.

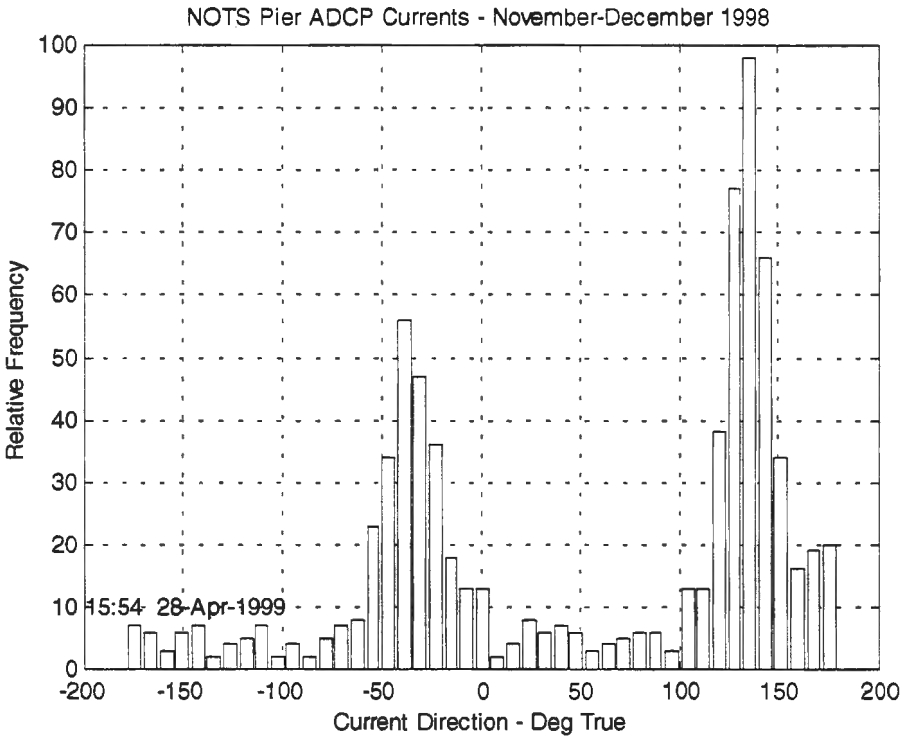

Figure 14. Histogram of ADCP Current Direction

The histogram shows that the main flow direction is to the southeast, with a secondary peak to the northwest. These directions are approximately parallel to the local coastline and isobaths. They are also perpendicular to NOTS Pier, where the direction of the long axis is 44° true. The measured velocities have been transformed into a coordinate system with axes parallel (positive offshore) and perpendicular (positive to the southeast) to the pier and plotted in figure 15, where they are labeled longshore and onshore. Vertical velocity (positive up) is included in the bottom panel at a scale 1/10 the horizontal components.

In the longshore/onshore coordinate system, nearly all the mean flow and tidal variability are in the longshore component. The mean velocity is to the southeast, increasing slightly from the upper layer to the bottom layer. Conversely, the rms longshore velocity decreases with increasing depth. The mean onshore/offshore velocity is in the offshore direction with the maximum flow in the bottom layer. This mean outflow near the bottom is required to balance the radiation transport toward the shore by the surface waves. Vertical velocities are very small, but also achieve their maximum (negative) value in the bottom layer, corresponding to a downward flow. This vertical velocity may be due to the net outflow on the steeply sloping bottom. The ratio of the mean downward flow to the mean outward flow in the bottom layer is equivalent to a slope of 12°. Velocity spectra for each of the components have been calculated and are plotted in figure 16. Diurnal tides dominate all but the vertical velocity, and there are several strong tidal harmonics. In the longshore current, the diurnal band contains 47 percent of the variance, the semidiurnal has 35 percent, and higher frequencies have the rest. Obviously,

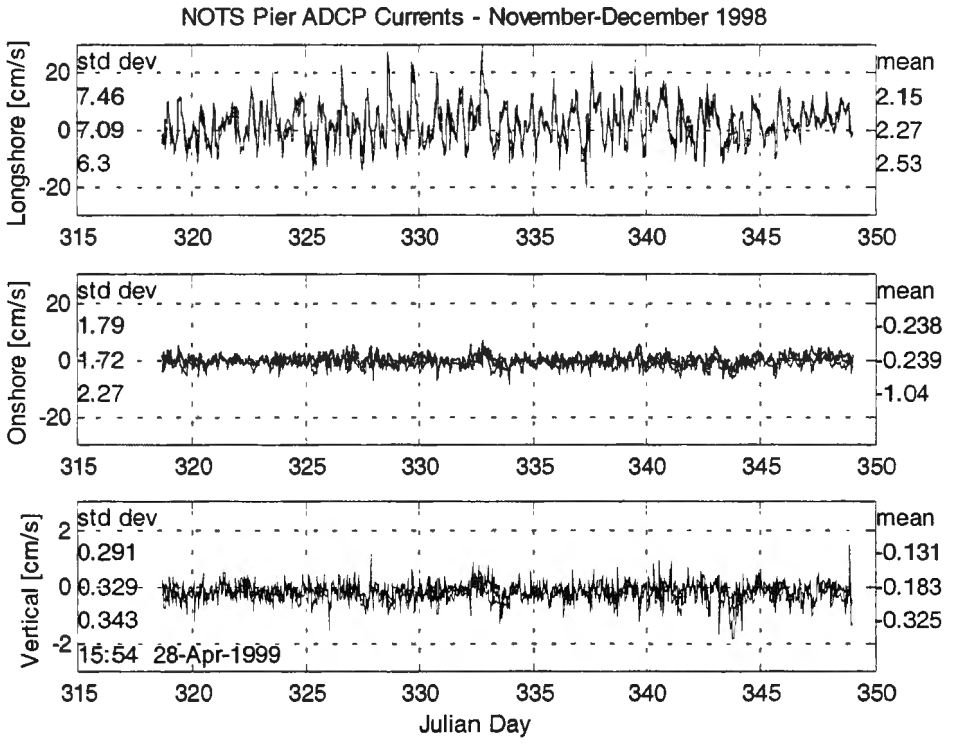

Figure 15. NOTS Pier ADCP Currents Resolved into Longshore, Offshore, and Vertical Components

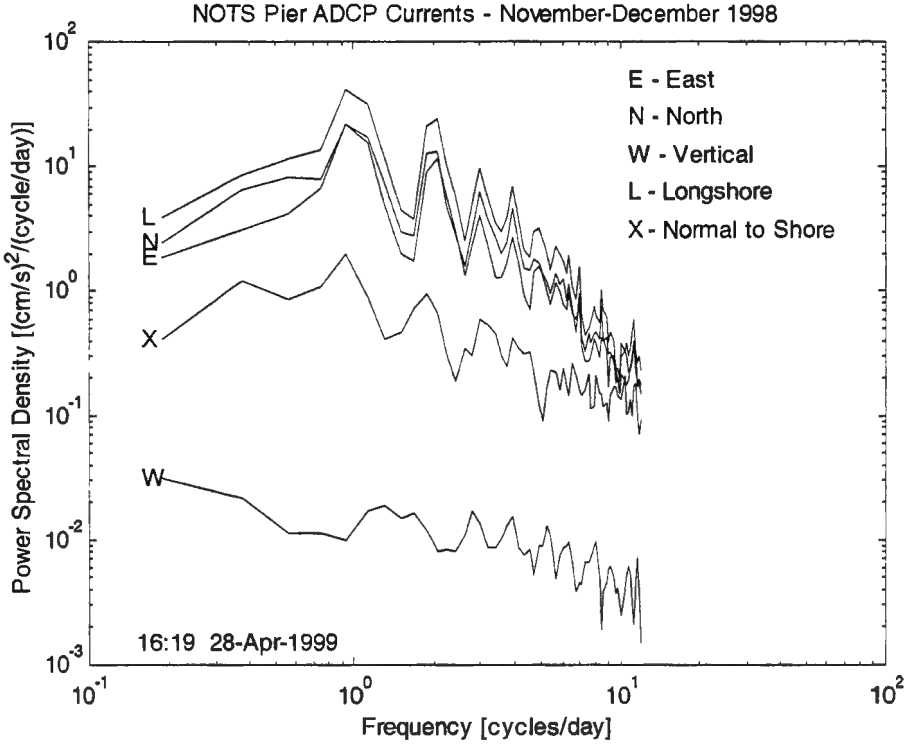

Figure 16. ADCP Velocity Spectra

most of the energy is in the longshore component as indicated by the time series plots. The overall picture of the currents at NOTS Pier from the ADCP measurements is a weak (~ 2 cm/s) mean flow to the southeast and a stronger (~ 8 cm/s rms) diurnal tidal current. Both the mean and tidal currents are parallel to the coast and perpendicular to NOTS Pier.

BOTTOM PRESSURE MEASUREMENTS

During the November through December 1998 test period, a Sea-Bird Electronics SBE 26 wave and tide recorder was deployed at a depth of 8.6 m near the seaward end of NOTS Pier. The instrument records integrated pressure at regular intervals to measure the tidal elevation in addition to bursts of high frequency (4 Hz) pressure data to estimate the surface wave height spectrum. The SBE 26 was programmed to record the average pressure every 6 minutes and a 1200-sample burst at 4 Hz every 6840 seconds. These data were used to compare the wave spectrum from a relatively long period (40 days) to the 1-day site survey to determine whether the latter measurements represent typical conditions. Figure 17 shows the average bottom pressure spectrum, labeled "Raw Pressure," for the period 6 November through 12 December 1998. The spectrum peaks at a frequency of 0.07 Hz to 0.08 Hz (period 12 s to 13 s) and falls off rapidly for frequencies greater than 0.2 Hz. The second curve in the plot, labeled "Depth Corrected," is an estimate of the surface wave height spectrum, using a correction factor for the bottom pressure measurements based on linear surface wave theory (see appendix). Briefly, the bottom pressure variations from the shorter waves, corresponding to the higher frequencies, are attenuated by the pressure response factor

$$K_p = \frac{1}{\cosh(kh)},$$

where k is the wave number, which must be computed from the dispersion relation, and h is the bottom depth. In the limit of long waves or shallow water $kh \rightarrow 0$, $\cosh(kh) \rightarrow 1$, there is no reduction in the pressure fluctuations. For shorter waves, the attenuation can become very significant. At the depth of the pressure gauge, $K_p = 1/10$ at $f = 0.3$ Hz, and the correction factor for the spectrum is $K_p^{-2} = 100$ (see the appendix for details). From these arguments, it appears that the bottom pressure measurements are useful only for frequencies less than 0.3 Hz because of the large correction factors needed at higher frequencies.

Figure 17 represents the average pressure spectrum for the 40-day deployment, but there was considerable variation in the wave climate during the period. This variability is illustrated in figure 18, where evolution of the spectrum is shown as a function of time. Each burst sample, separated by 114 min, is represented by an individual bottom pressure spectrum. The plots are limited to frequencies less than 0.3 Hz because of the large correction factors needed for higher frequencies. There are two views represented in figure 18: a contour plot that is useful for

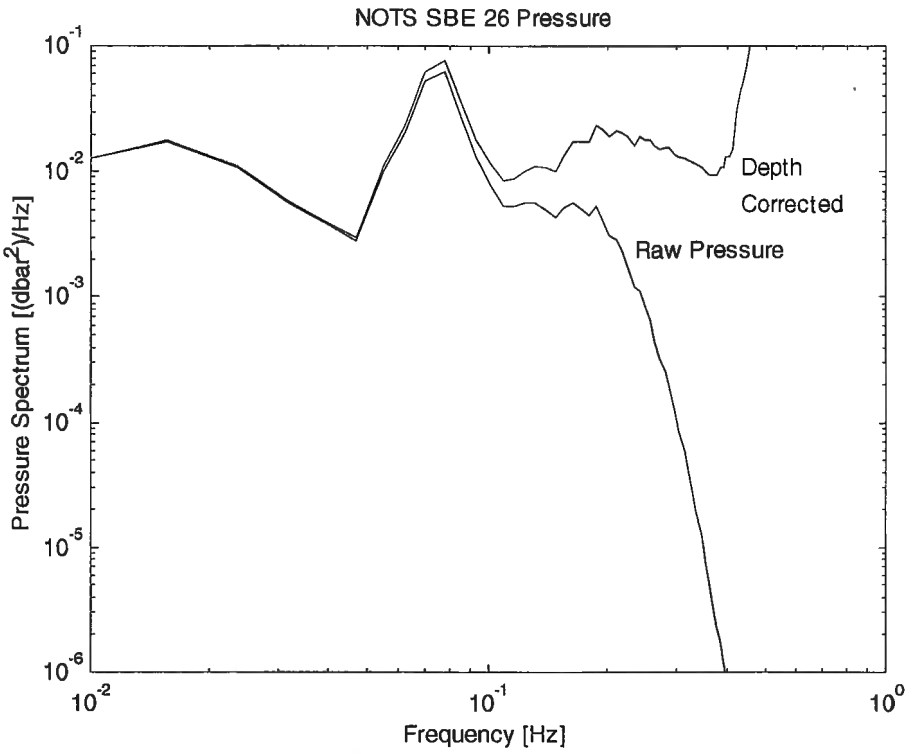

Figure 17. Bottom Pressure Spectra

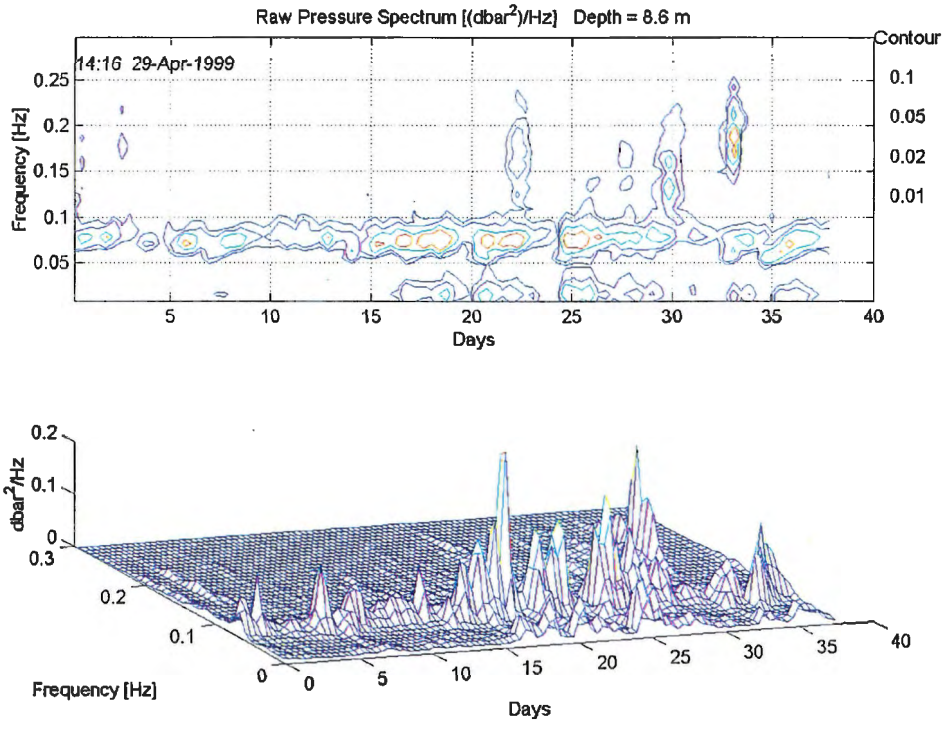

Figure 18. Time History of Bottom Pressure Spectrum

estimating numerical values and a three-dimensional plot that gives a clearer picture of trends. The comparable plot for surface wave height at the pressure recorder location, using the correction for attenuation for a depth of 8.565 m determined from the average pressure, is shown in figure 19. These figures show that the swell, with a period of about 12 s to 13 s, is a consistent feature in the spectrum and higher frequency waves are sporadic. The dominant swell period in these data is somewhat longer than the 10-s period observed in the 25 January 1999 site survey, but this longer period may be due to seasonal variations.

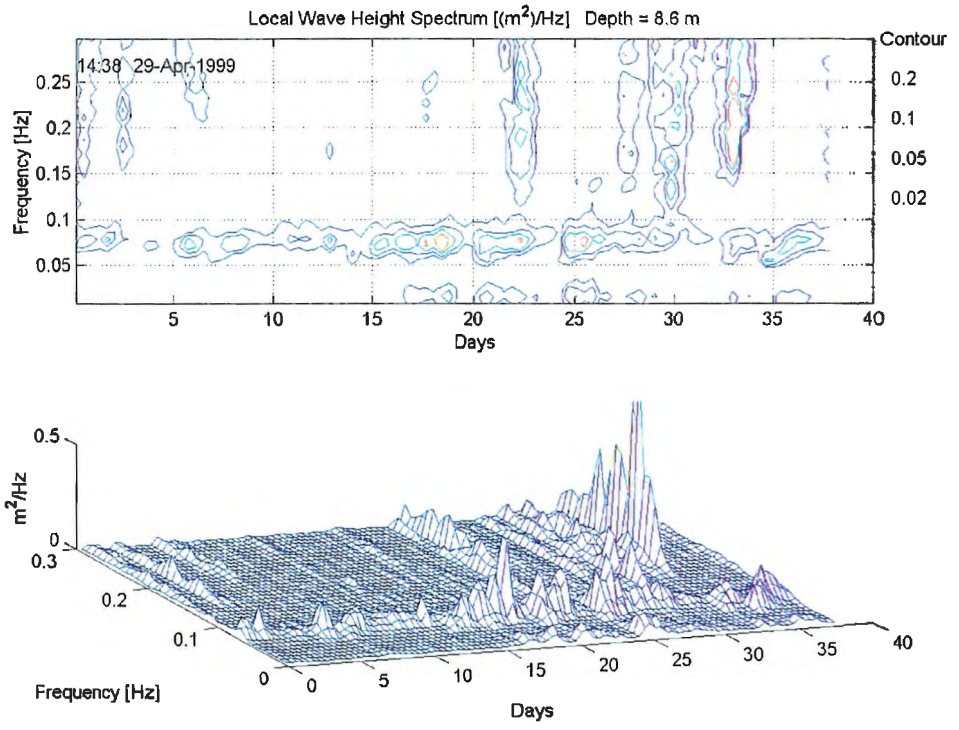

Figure 19. Time History of Wave Height Spectrum at Wave Recorder Location

Shoaling waves change their wavelength and wave amplitude, but they do not change their period. With this fact, combined with linear wave theory, the velocities induced by waves at any location after the wave height spectrum at any other location and depths at both locations are known can be predicted (see the appendix for details). Thus the bottom pressure measurements off NOTS Pier can be used to compute the wave height spectrum at the location of the pressure measurements, which, in turn, predicts the wave-induced velocities at any specific location (bottom depth) and sensor depth under the pier. Figures 20 and 21 show the predicted time history of horizontal and vertical velocity spectra, derived from the offshore bottom pressure measurements, at a sensor depth of 10 ft, where the water depth is 20 ft. Finally, the time histories of horizontal and vertical rms velocities in two bands, $T > 10$ s and $3.3 < T < 10$ s, are plotted in figure 22 at this location. These plots show that the rms horizontal velocity of approximately 5 cm/s and vertical velocity of about 1 cm/s observed during the very short measurement period on the 25 January 1999 site survey are typical of quiet winter conditions at NOTS Pier; they also provide estimates of the variability that can be expected to be encountered at NOTS Pier over longer time periods.

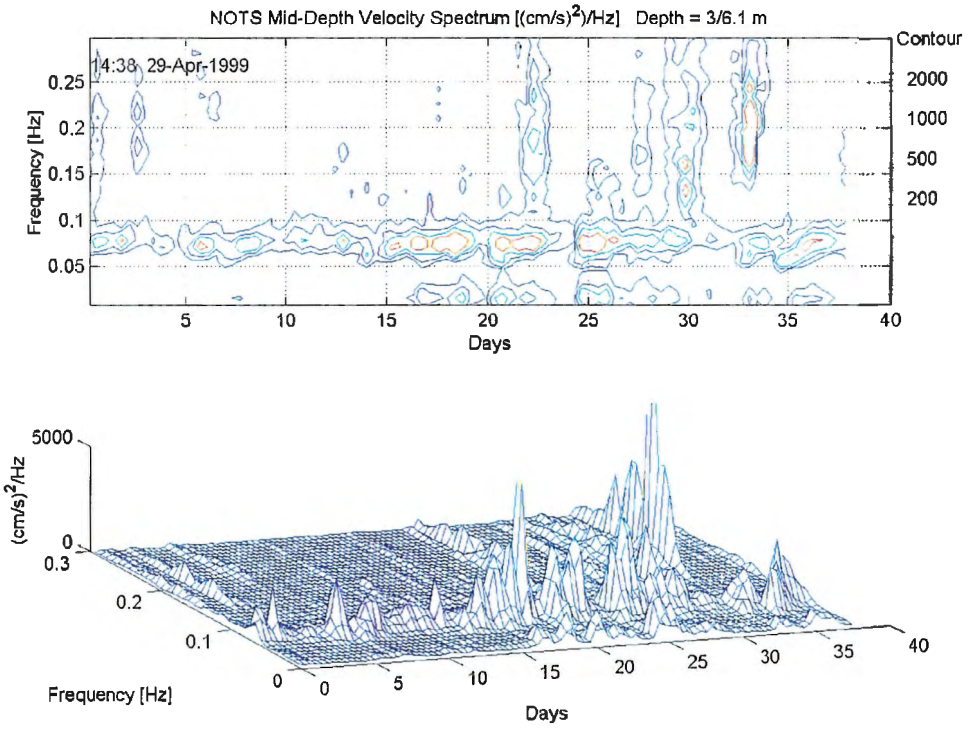

Figure 20. Wave-Induced Horizontal Velocity at Mid-Depth at NOTS Pier

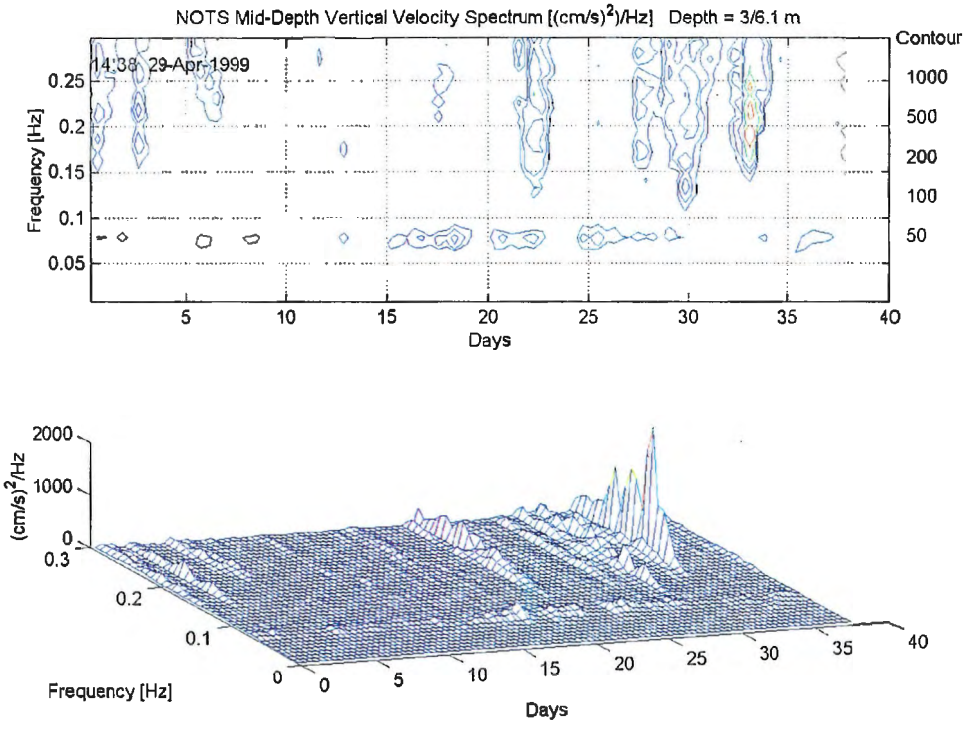

Figure 21. Wave-Induced Vertical Velocity at Mid-Depth at NOTS Pier

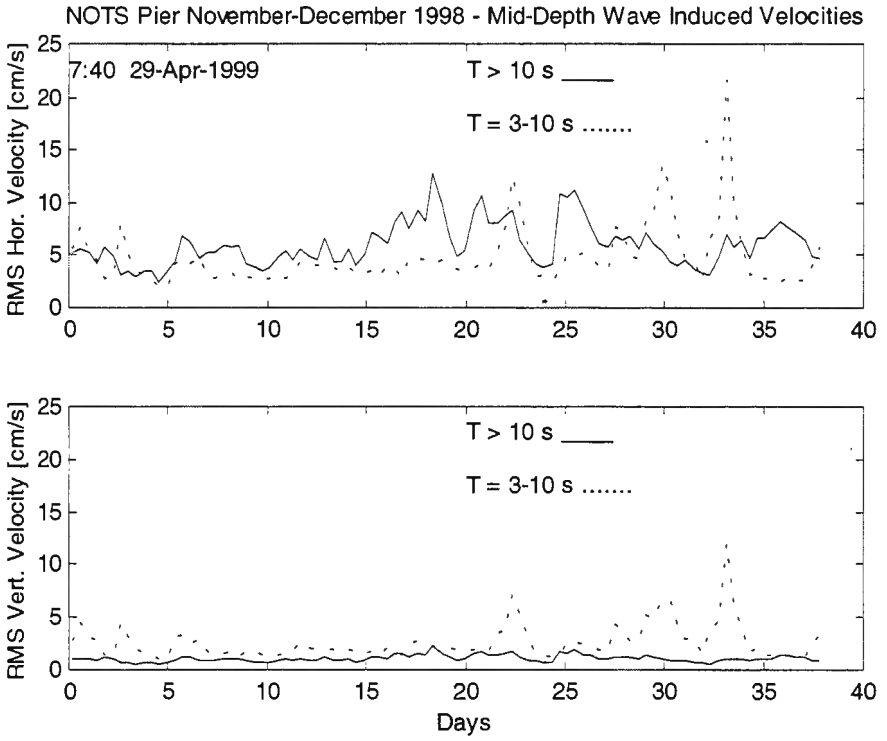

Figure 22. Time History of Wave-Induced rms Velocity at Mid-Depth at NOTS Pier

SUMMARY AND CONCLUSIONS

A 1-day survey of oceanographic conditions at NOTS Pier on San Clemente Island, CA, was conducted on 25 January 1999 to assess the suitability of this site for testing ocean turbulence sensors. Based on the measurements from two high-sample-rate current meters suspended from NOTS Pier, the survey showed that the mean currents were weak, but waves attributed to ocean swell, with a period of 10 s, produced horizontal oscillations with an rms amplitude of approximately 5 cm/s. Vertical velocity fluctuations were weaker, decreasing with increasing depth, and included shorter periods associated with wind waves, rather than swell. Variability in the velocities at higher frequencies ($0.5 < f < 4$ Hz) had continuous power spectra that are consistent with anisotropic turbulence with a dissipation rate $\varepsilon_u = 1.1 \times 10^{-5}$ m^2/s^3 based on the horizontal velocity spectrum and $\varepsilon_w = 1.1 \times 10^{-6}$ m^2/s^3 based on the vertical spectrum. Turbulent velocities associated with these dissipation rates in the frequency band ($0.1 < f < 4$ Hz) were approximately 1 and 0.4 cm/s for the horizontal and vertical components, respectively.

Another more extensive oceanographic survey was conducted at NOTS Pier in November-December 1998. Analysis of a 30-day-long record from a bottom-mounted acoustic Doppler current profiler 30 m off the end of the NOTS Pier in 15 to 20 m of water shows that currents are predominantly tidal and parallel to the coastline and local isobaths. For the 1-month period, the rms amplitude was approximately 8 cm/s with a peak current of 25 cm/s. The mean

current was approximately 2 cm/s to the southeast, also parallel to the isobaths and the coastline. The currents were essentially barotropic (independent of depth) and horizontal.

The latter data set included a record from a bottom-mounted pressure gauge located at a depth of approximately 8.5 m off NOTS Pier. These offshore bottom pressure measurements can be used to predict wave-induced velocities under the pier using linear surface wave theory. The pressure measurements span a 40-day period in November-December 1998. The period of the swell observed in the pressure gauge measurements was longer (12 s vs. 10 s) than that observed in the current meter data. The horizontal velocity amplitudes derived from the pressure gauge record during quiet periods were comparable (approximately 5 cm/s rms) to the velocities measured directly with current meters in the 1-day survey. Several energetic events in the pressure record (probably associated with storms) had much larger (approximately 10 to 20 cm/s rms) horizontal and vertical velocities because of short-period (3- to 5-s) wind waves. These data from a much longer time period confirm that the direct measurements of wave-induced velocities, collected during the brief site survey with rapid sampling current meters, were typical of quiet winter conditions at the NOTS Pier site.

These data reported here have the following implications for testing ocean turbulence sensors at NOTS Pier on San Clemente Island:

- There will be a slowly varying (mainly diurnal) weak mean current 0 to 20 cm/s normal to the long axis of NOTS Pier. The long-term average current parallel to the pier will be a few cm/s or less.

- A higher frequency current oscillation from surface waves with periods of 3 to 12 s will have amplitudes of 5 cm/s or more. The direction of these currents will be aligned with the swell, which will probably be onshore-offshore, parallel to the pier.

- The displacements (orbital motions of the water) will be on the order of the wave height (when wavelength/depth is nears 2π), which was about 10 cm during the January 1999 site survey.

- Experiments cannot depend on a quasi-steady mean current, but a regular sloshing action attributed to the swell can be expected. This sloshing, combined with a weak current, will create turbulence because of the interaction of the currents with the pier structures. The intensity of the turbulence will be proportional to the amplitude of the swell. The turbulence will exist at all depths near the pier and may be locally intensified near the surface or the bottom. Vertical velocities will be small (< 1 cm/s) except near the surface under larger, high-frequency (T < 10 s) wind waves.

REFERENCES

1. K. Vierra, "CSME Hydro 1.5 Data Logs and CD-ROM," Arété Associates (unpublished manuscript), Arlington, VA (UNCLASSIFIED).

2. G. Voulgaris and J.H. Trowbridge, "Evaluation of the Acoustic Doppler Velocimeter (ADV) for Turbulence Measurements," *Journal of Atmospheric and Oceanic Technology*, vol. 15, 1998, pp. 272-289.

3. P. Nasmyth, "Oceanic Turbulence," Ph.D. Dissertation, University of British Columbia, 1970.

4. N. S. Oakey, "Determination of the Rate of Dissipation of Turbulent Energy from Simultaneous Temperature and Velocity Shear Microstructure Measurements," *Journal of Physical Oceanography*, vol. 12, 1982, pp. 256-271.

5. P. S. Eagelson and R. G. Dean, "Small Amplitude Wave Theory," in *Estuary and Coastline Hyrodynamics*, A. P. Ippen, ed., McGraw-Hill, New York, 1966.

APPENDIX
LINEAR SURFACE WAVES

Assume a two-dimensional surface wave field with waves traveling in the x-direction with the z-direction positive up and the origin at the mean water level. The bottom is at $z = -h$. Consider a progressive wave with wave height $\eta(x, t)$ at a location x is given by

$$\eta(x,t) = a \sin(kx - \omega t),$$

where a is the wave amplitude, $k = 2\pi/L$ is the horizontal waven umber, L is the wavelength, $\omega = 2\pi/T$ is the (radian) frequency, T is the period, and t is time. The velocity components $u(x, z, t)$ (horizontal) and $w(x, z, t)$ (vertical) are (reference 5)

$$u(x,z,t) = \frac{agk}{\omega} \frac{\cosh k(h+z)}{\cosh kh} \sin(kx - \omega t)$$

$$w(x,z,t) = -\frac{agk}{\omega} \frac{\sinh k(h+z)}{\cosh kh} \cos(kx - \omega t),$$

where g is the gravitational acceleration. Similarly, the pressure p is

$$p(x,z,t) = g\rho\left[a \frac{\cosh k(h+z)}{\cosh kh} \sin(kx - \omega t) - z\right],$$

where ρ is the fluid density, and the dispersion relation is

$$\omega^2 = gk \tanh(kh) \quad or \quad L = \frac{gT^2}{2\pi} \tanh \frac{2\pi h}{L}.$$

SHALLOW-WATER WAVES (LONG WAVES)

For deep-water waves, such as swell in the deep ocean, the depth is large compared to the wavelength, i.e., $kh >> 1$, $\tanh(kh) \rightarrow 1$, and the deep-water wavelength is

$$L_0 \rightarrow \frac{g}{2\pi}T^2.$$

At San Clemente Island, the period of the swell is observed to be $T \cong 10$ s. Thus, the deep-water wavelength is $L_0 = \frac{g}{2\pi}(10)^2 = 156\,m$. As the deep-water wave moves into shallow water, its properties, including wavelength, amplitude, and velocity change, but the period remains constant. For example, a 10-s wave has a wavelength one-half of its deep-water limit when the water depth is 6 m. At the observation points, where the water depth was 4 to 8 m, these deep-water waves have been transformed to shallow-water waves or long waves because their wavelength is greater than the water depth ($kh>>1$). Using this approximation for 10-s waves, $kh = 0.3$ to 0.6 for $-h = 4$-8 m, and the hyperbolic functions approach their shallow-water limits $\sinh(kh)\rightarrow kh$, $\cosh(kh)\rightarrow 1$, and $\tanh(kh)\rightarrow kh$. (The conventional limit for shallow-water waves is $kh < \pi/10$ (reference 5)). Then

$$u_1(x,t) = \frac{a_1 g k_1}{\omega}\sin(k_1 x - \omega t)$$

$$w_1(x,z,t) = -\frac{a_1 g k_1}{\omega}k_1(h+z)\cos(k_1 x - \omega t)$$

$$p_1(x,z,t) = g\rho\left[a_1 \sin(k_1 x - \omega t) - z\right] = p'_1(x,t) + p_0(z),$$

and the dispersion relation is $\omega^2 = ghk_1^2$ *or* $L_1^{\,2} = ghT^2$, where the subscipt "1" indicates local values of parameters transformed from their deep-water limits. From these expresions it is clear that the horizontal velocity and the fluctuating part of the pressure p_1' (neglecting the $g\rho z$ term) are independent of depth, while the amplitude of the vertical velocity decreases linearly with depth (z is negative below the mean water level). Computing the variance for the velocity and pressure fluctuations,

$$\sigma^2_{u_1} = \frac{a_1^{\,2} g^2 k_1^{\,2}}{2\omega^2} = \frac{a_1^{\,2} g}{2h}$$

$$\sigma^2_{w_1}(z,\omega) = \frac{a_1^{\,2} g^2 k_1^{\,2}}{2\omega^2}k_1^{\,2}(h+z)^2 = \frac{a_1^{\,2}\omega^2}{2h^2}(h+z)^2$$

$$\sigma^2_{p'_1} = \frac{a_1^{\,2} g^2 \rho^2}{2}.$$

These expressions for the velocity variance are valid only for waves that are long compared to the water depth because the shallow-water dispersion relation is used for the derivation. The result for pressure does not use the dispersion relation, but it does use the long-wave approximation for the hyperbolic cosine.

For the 10-s period swell at NOTS pier, where $-h \cong 6$ m, the measured values are $\sigma_u^2 \cong 25$ $(\text{cm/s})^2$, $\sigma_w^2 \cong 0.5$ $(\text{cm/s})^2$, and $\sigma_p^2 \cong 2 \times 10^{-5}$ $(\text{decibar})^2$. Solving for the wave amplitude in terms of these measured variances and assuming that the instruments were located at 40 – 70 percent of the water depth,

$$\textit{horizontal velocity}: \quad a_1 = \left(\frac{2\sigma_{u_1}^2 h}{g} \right)^{1/2} = 6.4\ cm$$

$$\textit{vertical velocity}: \quad a_1 = \frac{\left(\frac{\sigma_{w_1}^2 T^2}{2\pi^2} \right)^{1/2}}{(1+\frac{z}{h})} = \frac{1.6}{(1+\frac{z}{h})}\ cm = 5.3\ cm \ \textit{for}\ \frac{z}{h} = -0.7$$

$$\textit{pressure}: \quad a_1 = \left(\frac{2\sigma_{p_1}^2}{g^2 \rho^2} \right)^{1/2} = 6.3\ cm.$$

To be consistent, all three estimates should give the same wave amplitude. Given the uncertainties about the water depth, the depth of the instruments, and the calibration of the pressure sensor, these estimates are remarkably consistent. Furthermore, the long-wave approximation is marginally valid for 10-s waves in the assumed water depth.

DEEP-WATER WAVES (SHORT WAVES)

For the case of relatively short waves, $kh >> 1$, the bottom has no effect on the waves and the limiting forms of the hyperbolic functions are $\cosh(kh) \rightarrow e^{kh}/2$, $\sinh(kh) \rightarrow e^{kh}/2$, and $\tanh(kh) \rightarrow 1$, and the dispersion relation becomes $\omega^2 = gk$. Substituting,

$$u_s = \frac{agk}{\omega} e^{kz} \sin(kx - \omega t) = a\omega e^{kz} \sin(kx - \omega t)$$

$$w_s = \frac{agk}{\omega} e^{kz} \cos(kx - \omega t) = a\omega e^{kz} \cos(kx - \omega t)$$

$$p_s = a\rho g e^{kz}.$$

In the MAVS data, the vertical and horizontal spectra are equal at about 0.3 Hz, where the amplitude is approximately 5 $(cm/s)^2/Hz$. Using the variance $\sigma_w^2 = 0.9\ (cm/s)^2$ in the frequency band $0.2 < f < 0.4$ Hz, the short wave dispersion relation $kz = \omega^2 z/g$, $\omega = 2\pi/T \cong 2$ 1/s, and the depth of MAVS, z = -2.4 m,

$$a_u = a_w = \left(\frac{2\sigma_w^2}{\omega^2} \right)^{1/2} e^{-kz} = 1.8\ cm.$$

OFFSHORE BOTTOM PRESSURE MEASUREMENTS

From the original expression for pressure above, it is clear that the pressure at a point beneath a wave varies with the height of the water above that point. The pressure is linearly proportional to the waveheight, but it also depends on the bottom depth and the ratio of the depth to the wavelength of the wave. At the bottom, where the depth is $z = -h_0$, the pressure is

$$p_0(x,-h_0,t) = g\rho \left[a \frac{1}{\cosh kh_0} \sin(kx - \omega t) + h_0 \right].$$

This relationship between the pressure variations at the surface and the pressure at the bottom is given by the pressure response factor, K_p, which is defined as

$$K_p = \frac{1}{\cosh(kh)}.$$

For shallow water or long waves $kh \rightarrow 0$ and $\cosh(kh) \rightarrow 1$; for deep water or short waves, $kh \rightarrow \infty$ and $\cosh(kh) \rightarrow 0$. The bottom pressure record from a moored gauge is a function of time, not wave number, at a specific depth, and the associated power spectrum is a function of frequency. To use the pressure response factor to compute wave height as a function of frequency from bottom pressure, the dispersion relation, $\omega^2 = gk \tanh(kh_0)$, must be used to compute wave number as a function of frequency at a specific depth. The results of this wave number calculation and response function, $K_p(f = \omega/2\pi, h_0)$, are shown in figure A-1 for a bottom depth h_0 = 8.6 m, which was determined from the mean pressure from the recorder located off NOTS pier.

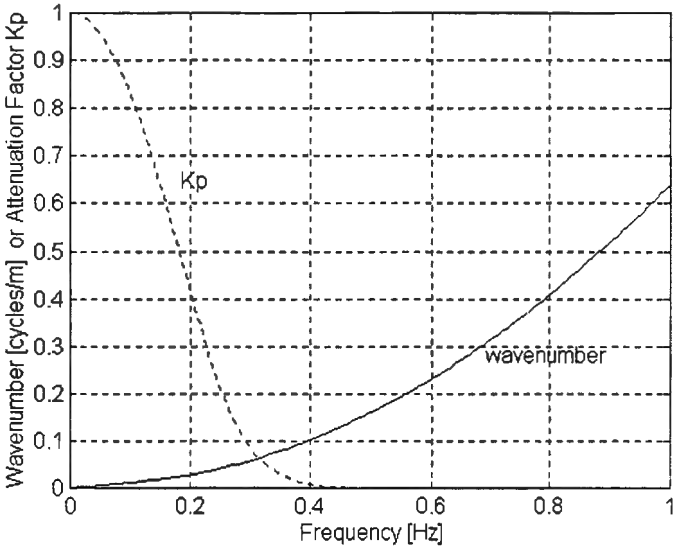

Figure A-1. Wave Number and Pressure Response Factor for 8.6-m Depth

From the figure it is clear that the pressure response factor decreases rapidly with frequency, reaching 1/10 at a frequency of 0.3 Hz where $k = 0.05$ cycles/m ($L = 20$ m). In terms of the power spectrum,

$$P_0(\omega) = g^2 \rho^2 K_p^2(\omega, h_0) \Theta_0(\omega),$$

where $P_0 = (\omega, h_0)$ is the bottom pressure spectrum and $\Theta_0(\omega)$ is the corresponding wave height spectrum. This relationship is used to compute the wave height spectrum, at the location of the bottom pressure measurements, from the bottom pressure data, with the caveat that the results will be suspect at high frequency where the pressure correction K_p^{-2} becomes very large.

After the wave height spectrum $\Theta_0(\omega)$ has been determined at one location, where the bottom depth $z = -h_0$ is known, the wave height spectrum and wave-induced velocity spectra can be computed at any other location where the bottom depth is known. For example, the horizontal velocity spectrum $U_0(\omega, h_0, z)$ at the surface ($z = 0$) where the bottom depth is h_0 is

$$U_0(\omega, h_0, 0) = \frac{g^2 k^2}{\omega^2} \Theta_0(\omega),$$

or the horizontal velocity spectrum at depth z in the same location is given by

$$U_0(\omega, h_0, z) = \frac{g^2 k^2}{\omega^2} \frac{\cosh^2 k(h_0 + z)}{\cosh^2 (kh_0)} \Theta_0(\omega) .$$

At another location where the bottom depth is h_1, the local dispersion relation, $\omega^2 = gk \tanh(kh_1)$ is used to calculate the local wave height spectrum $\Theta_1(\omega)$ from $\Theta_0(\omega)$. From the local wave height spectrum, the horizontal velocity spectrum at the new location is, similarly,

$$U_1(\omega, h_1, z) = \frac{g^2 k^2}{\omega^2} \frac{\cosh^2 k(h_1 + z)}{\cosh^2 (kh_1)} \Theta_1(\omega) ,$$

or, for the vertical velocity,

$$W_1(\omega, h_1, z) = \frac{g^2 k^2}{\omega^2} \frac{\tanh^2 k(h_1 + z)}{\cosh^2 (kh_1)} \Theta_1(\omega) .$$

INITIAL DISTRIBUTION LIST

Addressee	No. of Copies
Office of Naval Research (ONR321SI (D. Johnson), ONR333 (S. Lekoudis, P. Purtell))	3
Center for Naval Analyses	1
Defense Technical Information Center	2